Gulf Journal of Engineering & Technology
FE Gulf Publishers
https://fegulf.com

# Artificial intelligence analysis of corrosion behavior of H59 brass alloy in red sea conditions with and without ceramic coating

Obaid Saleh Ba Yuosef[1], Mohmmad Salah Eldin Haij[2], Abdulmajeed Sami Alnemry[3], Ammar Ahmed Holbah[4], Mohammed Fahmi Lathkani[5], Ibrahim Sahban Abuhayyah[6], Abdulaziz mahdi alameer[7], Turki Nasser Jraba[8], Haitham Hadidi[9], Rajasekaran Saminathan[10] & Divya Raju[11]

[1-10] Department of Mechanical Engineering, College of Engineering and Computer Science, Jazan University, Saudi Arabia.
[11]College of Applied Health Sciences and Nursing, Jazan university, Saudi Arabia

**Corresponding Author**: Rajasekaran Saminathan
**Corresponding Author Email**: rsaminathan@jazanu.edu.sa

**Article Info**

**Volume No:** 1 **Issue No:** 3 **Page No:** 71-81

**Received:** 20-01-25 **Accepted:** 05-04-25 **Published:** 20-04-25

**Abstract**
Due to its exceptional resistance to corrosion, H59 is a marine grade alloy that is utilized widely in the maritime industry for a variety of applications throughout the industry. A scant amount of research has been done on the effects of heat treatment and ceramic coatings such as ceria on the corrosion behavior of H59 in conditions similar to those found in the Red Sea. This study aims to investigate the influence of heat treatment at temperatures of 200, 360, and 600 degrees Celsius over a range of time periods, as well as the application of a cerium oxide coating using the chemical bath technique, on the corrosion behavior of H59 alloy under conditions that are typical of the Red Sea. Furthermore, in order to acquire the artificial intelligence algorithm, the corrosion data of the alloy that has been exposed to heat treatment and surface coating is analyzed by the software that utilizes both machine learning and artificial intelligence. Heat treatment causes topographical changes in grain structures and results in the production of a metallic oxide layer on the surface of the alloy. The machine learning treatment has led to the identification of the quenching treatment at 600 and 200 degrees Celsius, as well as the annealing treatment at 360 degrees Celsius contribute to a greater corrosion rate with severity level 1. The coating made of cerium oxide has resulted in a reduction in the rate of corrosion to a level that is two times lower. .

**Keywords:** H59 Alloy, Corrosion Behavior, Red Sea, Heat Treatment, Artificial Intelligence, Machine Learning.

## INTRODUCTION

In general, metallic alloys are subjected to heat treatments, which include soaking treatment, which involves keeping the alloys at a specific temperature for a predetermined amount of time, and then proceeding with either quenching treatment or air cooling, depending on the requirements of the mechanical properties that need to be tailored (Gaurav & Shrikant, 2014; Loganathan, Gnanavelbabu, & Rajkumar, 2014; Gale & Totemeier, 2004). Copper alloys are among the most significant classes of alloy systems that are now accessible. They have a wide range of uses in a variety of sectors, including the electrical industry, the automotive industry, the aerospace industry, and desalination plants (Zeng, Chen, & Shun, 2014; Ronald & Ahmed, 2017; Kazunari, Yuki, & Hirotaka, 2013). When it comes to finding applications in heat transfer systems, such as heat sink pipes used in desalination units, H59 Brass alloy is one of the leading contenders (Pike-Wilson & Karayiannis, 2014; Satish, Srinaivas, & Dongqing, 2006). Indeed, the heat treatment of the copper-based alloy caused a change in the mechanical characteristics of the material. This change was brought about by the introduction of stacking fault energies, dislocations, and precipitates of alloying elements (Zhang, Yang, & Chen, 2016; Meyers, Vohringer, & Lubarda, 2001). In general, the microstructural characteristics of alloys are altered as a result of heat treatment and the addition of alloying materials. As a consequence, the corrosion behavior of the alloy undergoes significant evolution as a result of these modifications. This holds true for the alloys that are based on copper as well (Sunday, Sunday, & Tien-Chien, 2023; Noor, Abadlwahid, & Ali, 2020). Over time, the corrosion behavior of heat-treated alloys has been seen to deteriorate for a variety of causes, including the production of precipitates of alloying elements and changes in the grain structures of the alloy. This phenomenon has been observed in numerous instances. As a result, a great number of studies are focused on modifying the corrosion behavior of alloys by applying protective coatings or producing an oxide layer by laser treatment, among other methods (Hussein, Khalid, & Wasan, 2019; Emily & Marc, 2011; Xizhao, Lei, & Binggong, 2020; Liu, Ma, & Yang, 2022; Xinyi, Yue, & Zhonghao, 2021). Furthermore, the corrosion behavior of technical alloys under circumstances similar to those found in the Red Sea has not been well investigated and documented in the literature (Yahya, Ali, & Rajasekaran, 2020; Haitham, Rajasekaran, & Nasser, 2024). In recent years, the application of artificial intelligence to the analysis of corrosion data has resulted in the successful identification of important and non-critical parameters that influence the interdependency of one component with other ones. Therefore, this opens the door to the possibility of establishing an efficient maintenance routine for the structures that are used in engineering applications (Coehlho, Zhang, Van Ingelgem, 2022; & Rajasekaran, Abdulla, Abdulrahman, 2024). The results of the survey make it abundantly evident that there is room for research into the impact of heat treatment on the corrosion behavior of H59 brass alloy in circumstances of the Red Sea, along with the potential for the use of artificial intelligence software analysis.

## MATERIALS AND METHODS

H59 brass of diameter 1 cm is received and cut into small specimens of length nearly 2 cm. The cut specimens are polished using polishing sheets (SiC) of various grades up to 2000 grit. Then the polished specimens were subjected to diamond paste polishing using 3 µm diamond paste. The lengths and surface are of every specimen were then calculated accurately after measurements using vernier calliper. The polished specimens were then heat treated at various temperatures namely 200 360 and 600 $^{0}$C for a time period of 1 hour. Upon completing the heat treatment, the cooling process were carried out in two different roots. Few specimens were subjected to quenching in water where as other specimens were cooled in air. This is followed for all categories of the temperature. Further these specimens are subjected to hardness measurements using a Vickers microhardness measurement machine. After the hardness measurements corrosion testing is carried out by gravimetric analysis method. Every weighed specimen with weight (W1) immersed in a 500 ml of Red Sea Water collected 10 km away from the beach of Jazan region to ensure the sea water is not contaminated by human life at the beach. The gravimetric analysis is done at two phases namely after 5 weeks and 10 weeks. After removal from the sea water the specimens were cleaned chemically at a temperature of 70 $^{0}$C using a chemical bath containing 3 wt% $Cr_2O_3$ and 5 % $H_3$ $PO_4$ prepared with distilled water. The cleaning process involves introducing the specimen removed from sea water to the chemical bath maintained at 70 $^{0}$C for 10 seconds and then washed in running water. The specimens were then dried and weighed ($W_2$). The corrosion rates were calculated using the following formula [23],

$$Corrosion\ Rate\ (mpy) = \frac{KxW}{DxAxT}$$

Where

K= Constant (3.45 x $10^6$)
W = Weight Loss (g)
D- Density of Specimen (grams/cm$^3$)
A- Area of the specimen (cm$^2$)
T-Time of exposure in hours.

The corrosion rate data and the corresponding hardness data are combinedly fed to the artificial intelligence software to write the artificial intelligence algorithm. Following a chemical pretreatment process, the previously treated samples were immersed in a cerium solution to generate an oxide coating based on cerium. A duration of immersion is 30 minutes at a temperature of 30 degrees Celsius. The pH of the solution had been adjusted to 2.85 using NaAc + HAc and was maintained at a consistent level through the entire coating procedures. Distilled water was used to rinse after each process, including pretreatment and conversion. A bath solution was obtained by dispersing 7.5 g of $CeCl_3$ in 1000 ml of distilled water with a quantity of $H_2O_2$ (Ce : $H_2O_2$ molar ratio of 1 : 50) of 100 ml/L. The pre-processed samples were soaked in the coating solution for a duration of 30 minutes and then dried. The specimens used in this study and the Vickers hardness testing impression on the specimen are shown in Fig.1 and Fig.2.

Figure 1: The Specimens Used

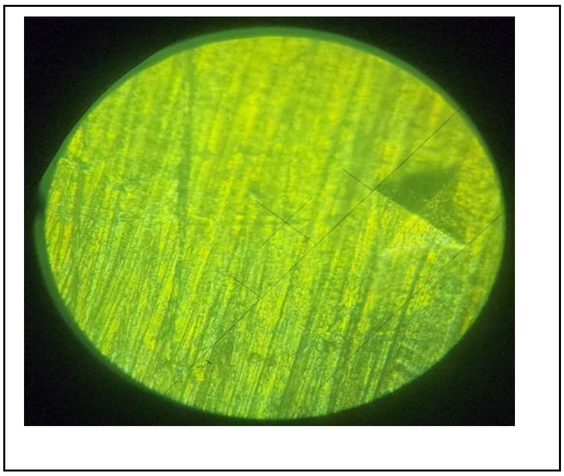

Figure 2: The Hardness Test Impression

## RESULTS AND DISCUSSION

Table 1 shows the corrosion data with corresponding hardness values H59 alloy subjected to heat treatment. The Q represents "quenched" and A represents "Air-cooled". The first impression of the table analysis indicates that as the temperature of heat treatment increases the hardness value increases. This is clearly visible in the case of quenched specimens indicating that the heat treatment has greater effect on the hardness variations when the specimens were quenched after heating process. Air cooling leads to a marginal increase in hardness values.

Table 1
*Hardness and Corrosion Data of h59 Brass Alloy*

| Specimen | Hardness (HV) | Corrosion Rate (mpy) |
|---|---|---|
| As resived | 48.9 | 0.45 |
| 200A | 46.5 | 0.33 |
| 200Q | 49.5 | 0.74 |
| 360A | 48.2 | 0.58 |
| 360Q | 51.2 | 0.65 |
| 600A | 49.98 | 0.51 |
| 600Q | 55.9 | 0.75 |
| Ceramic Coated | 52.3 | 0.21 |

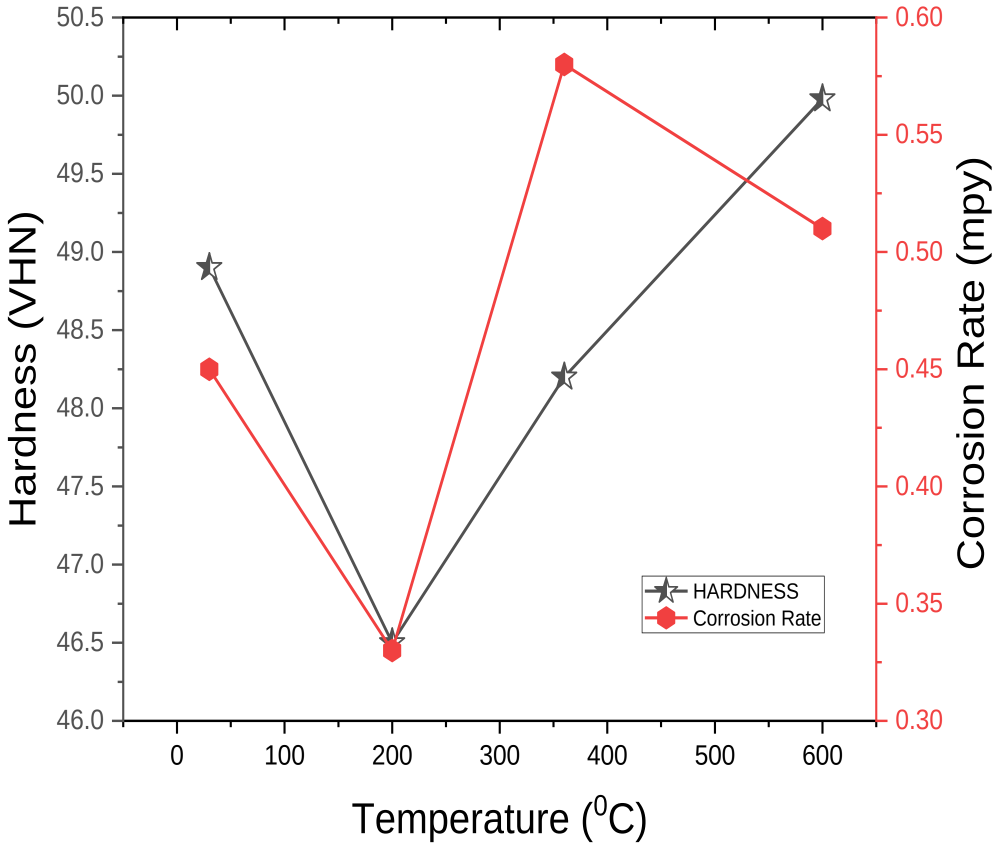


Figure 3: Hardness and Corrosion Rate Variation with Temperature for Air Cooling Mode

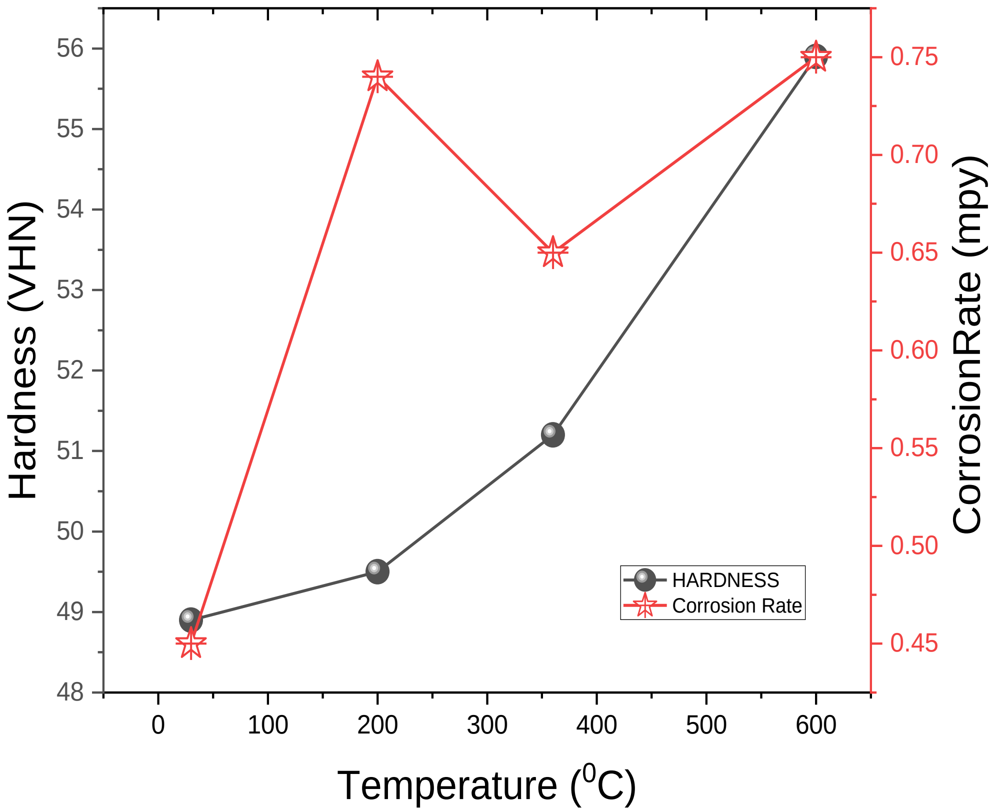


Figure 4: Hardness and Corrosion Rate Variation with Temperature for Quenching Mode

Similarly, the corrosion rate of the heat-treated specimens increases when there is an increase in heat treatment temperature. A careful examination indicates that the quenched specimens show greater tendency to the corrode in red sea water when compared to that of other group of specimens. The variations of corrosion rate with hardness variations corresponding to the heat treatment temperatures are shown in the following figures Fig 3 and 4. In the case of air cooling the hardness and corrosion rate follow similar trend where as in the case of quenching, irrespective of the heat treatment temperature the corrosion rates fall to the higher side with minimal variations.

Fig. 5 show the artificial intelligence algorithm of the hardness and corrosion data obtained in this research. The algorithm chooses the corrosion rate as the target parameter for the analysis. The critical corrosion rate is 0.39 mpy. For the category less than 0.39 directly corelates to the weight after immersion indicating that $W_2$ as the key factor (In second leaf) for specimens exhibiting corrosion rate less than 0.39. Moreover, the critical value of $W_2$ is 12.52.

The proceeding leaf connects the specimen categorisation in leaf 3 and identifies the heat treatment at 200 and 300 $^0$C as the influencing processes in deciding the corrosion rate of the specimens. The criticality of corrosion rate goes to the values of 0.39 and above directly related to the weight difference in the second leaf indication that WD less than 0.1 influenced by the W2 having a critical value of 12.45. In the third leaf it connects to the specimen categorisation showing the severity l for the specimen heat treated at 600 $^0$C and quenched in water. The leaf three incorporates the factor time of immersion having a critical value of 1260 hours. The corresponding leaf 4 incorporates $W_2$ having a critical value of 12.36 for the time of immersion having a value less than 1260 hours. If the time of immersion is more than 1260 hours then the corrosion rate will be automatically higher than 0.51.

In order to offer a visual representation of the qualitative knowledge of the distribution, it is feasible to plot the distribution of each characteristic with respect to other in attribution analysis. It is crucial to observe the colours red and blue, which denote the positive and negative classes, respectively. A colour is automatically assigned to each category value in order to align with it. If there were three categories for the class value, the pre distribution would be divided into three hues, rather than two. It is beneficial to quickly assess whether the parameters can be easily divided by a specific attribute, such as when all of the red and blue are cleanly separated for a single attribute.

The parameter which is critical among the selected parameters, as evidenced by the overlapping of positive and negative leaves in the attribution analysis (Fig.6). It is necessary to target the critical one for further analysis of AI. The attribution analysis clearly shows the overlapping in the case of corrosion rate.

In order to ensure that the data is compatible with the Artificial Intelligence Analysis Software (AIS), it is imperative to convert it to a specific format. The final stage in the process of creating the Artificial Intelligence Algorithm (AIA) is to conduct additional categorization of the numerous parameters that have been designated as objectives. This is necessary to complete the operation that has been initiated. The Artificial Intelligence Analysis (AIA) is responsible for conducting an analysis of the impact of each parameter on the experimental data that is associated with the target parameters that have been predetermined. The J48 algorithm and the random tree-based approach both have the potential to be successful in attaining success in each and every set of objectives. The output data that indicates the accuracy of the classification includes the F-measure, the Mathew Correlation Coefficient (MCC), the TP rate (True Positive Rate), the FP rate (False Positive Rate), the ROC (Receiver Operating characteristics) area, and the PRC area. The ROC area and the PRC (Precision Recall Curve) area are additional examples. In a manner that is both effective and efficient, the algorithm is capable of identifying the variability in the parameters associated with the influencing parameters causing maximum corrosion of the heat treated H59 brass. Naïve Bayes classifier analysis prove that the AI test run is valid and hence the criticality factors are identified correctly.

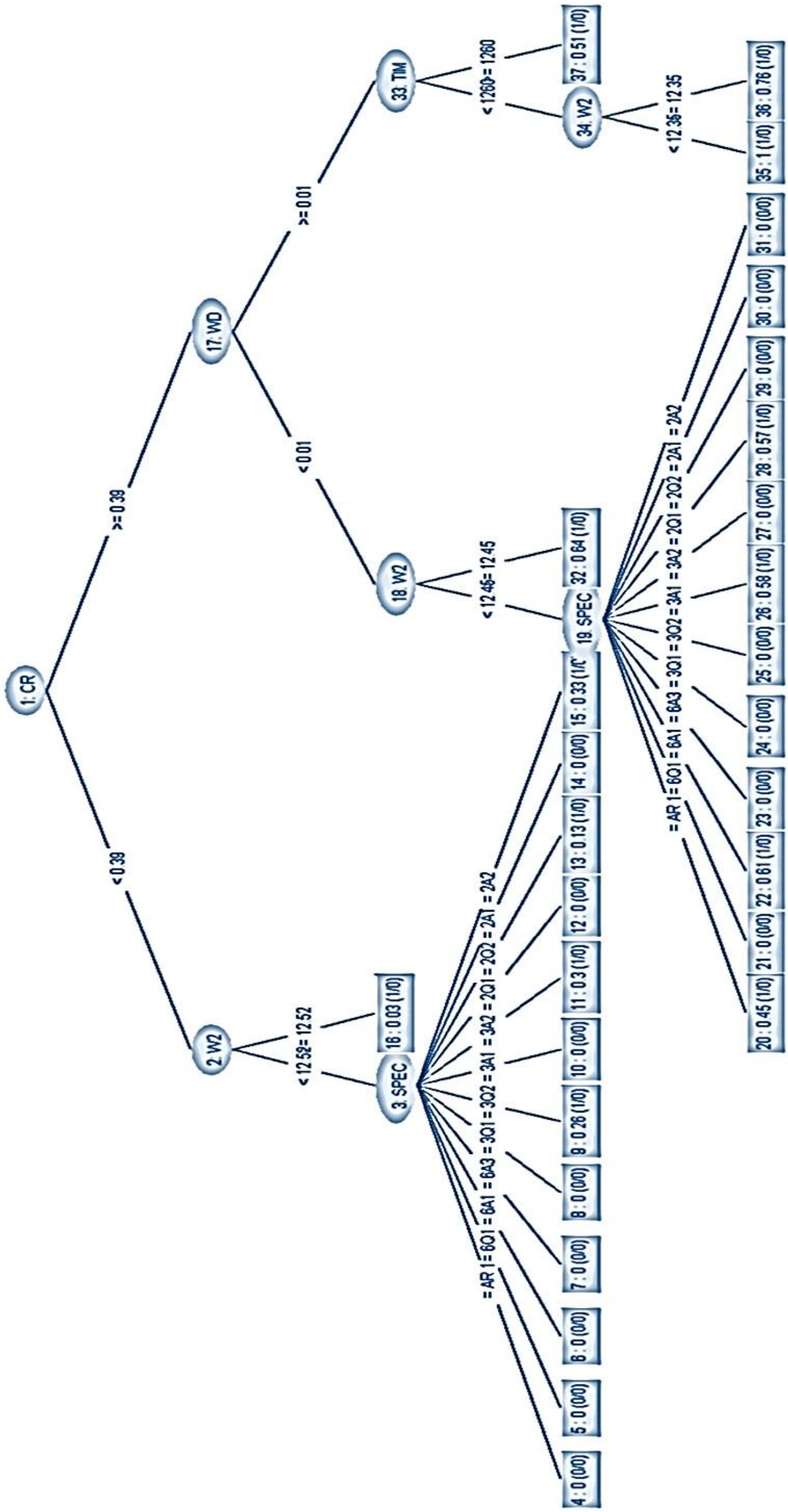


*Figure 5: Machine Learning Algorithm of the Corrosion Behaviour of the H59 Alloy*

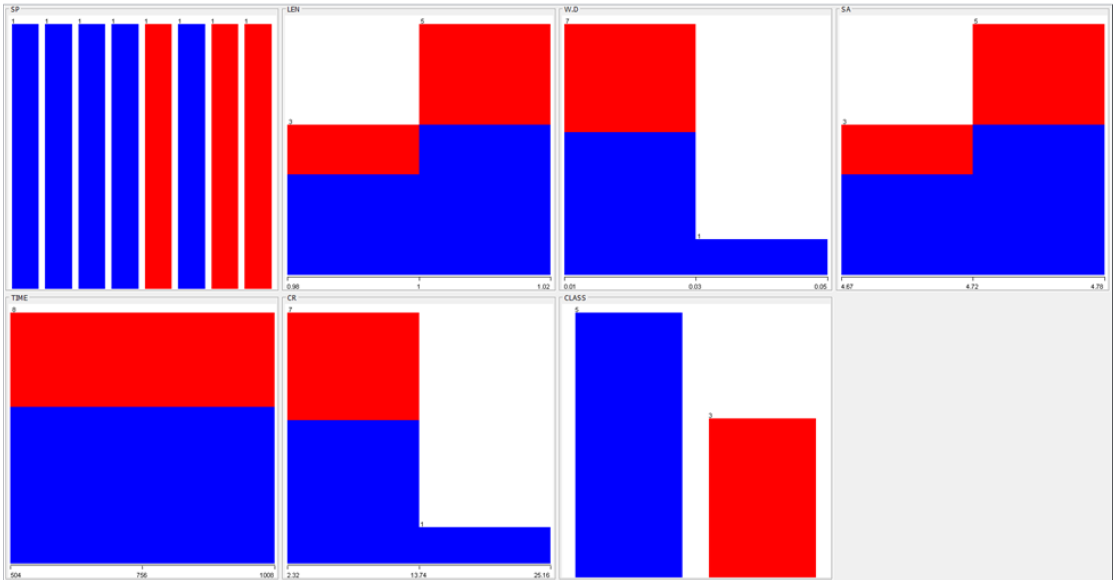


Figure 6: Attribution Analysis of Artificial Intelligence Test Run

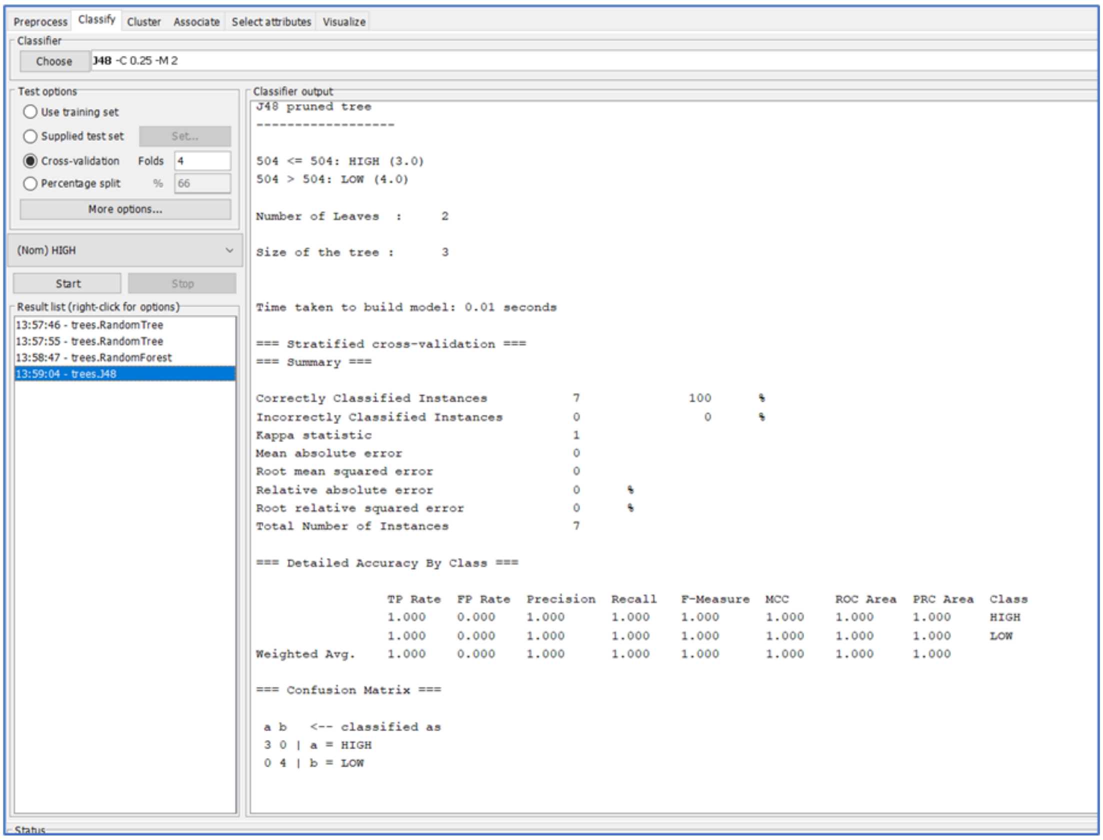


Figure 7: The Output of Machine Learning Algorithm with Naïve Bayes Classifier Regulations

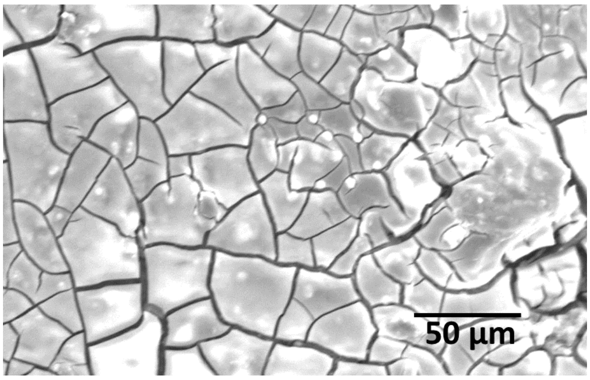


Figure 8: The Ceria Coating on the H59 Alloy

Figure 8 shows the cerium oxide coating on the H59 alloy. Even though it looks like crack bound one, the surface of the H59 alloy is completely coated with Ceria layer indicating the uniformity of coating presence. Hence when exposed to the red sea water the ceria layer protects the alloys surface from corrosion.

## CONCLUSIONS

The influence of heat treatment on the corrosion behaviour of the H59 alloy in red sea conditions is studied successfully. The heat treatment reveals that the specimens heated at 600 $^{0}$C for 1 hour and water quenched show higher hardness as well as increased tendency to corrode in red sea water when compared to the other group of specimens. The artificial intelligence analysis identifies the critical range of corrosion rate as 0.39 mpy and it is corelated to the hardness, weight difference in gravimetric analysis and time of immersion. The cerium oxide coating proves very effective by reducing the corrosion rate of the H59 alloy to nearly less than 50 %.

## References

Coelho, L. B., Zhang, D., Van Ingelgem, Y., et al. (2022). Reviewing machine learning of corrosion prediction in a data-oriented perspective. *NPJ Materials Degradation*, *6*, 8. https://doi.org/10.1038/s41529-022-00218-4

Emily, S., & Marc, E. (2011). Effects of flow, brass location, tube materials and temperature on corrosion of brass plumbing devices. *Corrosion Science*, *53*(5), 1813–1824. https://doi.org/10.1016/j.corsci.2011.01.060

Gale, W. F., & Totemeier, T. C. (2004). Heat treatment. In *Smithells Metals Reference Book* (8th ed.). Butterworth-Heinemann. https://doi.org/10.1016/B978-075067509-3/50032-4

Gaurav, D. S., & Shrikant, U. G. (2014). Review on recent trends & optimization in heat treatment. *International Organization of Scientific Research*, *11*, 52–58. https://doi.org/10.9790/1684-11365258

Haitham, H., Rajasekaran, S., & Nasser, Z. (2024). Enhancement of diffusive oxidation resistance and topographical corrosion resistance of hot work tool steels by nickel multifunctional coatings. *Journal of Materials Research and Technology*, *28*, 1227–1232. https://doi.org/10.1016/j.jmrt.2023.12.052

Hussein, Y. M., Khalid, A. S., & Wasan, K. M. (2019). Corrosion protect of brass tubes heat exchanger by using CuO nanocoating with thermal pyrolysis techniques. *Journal of Mechanics of Continua and Mathematical Sciences*, *14*(4), 281–291. https://doi.org/10.26782/jmcms.2019.08.00023

Kazunari, M., Yuki, I., Hirotaka, M., et al. (2013). Solid-solution copper alloys with high strength and high electrical conductivity. *Scripta Materialia*, *68*(10), 777–780. https://doi.org/10.1016/j.scriptamat.2012.12.027

Liu, L. H., Ma, H. W., Yang, S. J., et al. (2022). Decomposition of cellular structure in selective laser melted Cu–Zn–Si silicon brass and its influence on microstructure, mechanical and corrosion properties. *Materials Science and Engineering: A*, *841*, 143055. https://doi.org/10.1016/j.msea.2022.143055

Loganathan, D., Gnanavelbabu, A., Rajkumar, K., et al. (2014). Effect of microwave heat treatment on mechanical properties of AA6061 sheet metal. *Procedia Engineering*, *97*, 1692–1697. https://doi.org/10.1016/j.proeng.2014.12.320

Meyers, M. A., Vöhringer, O., & Lubarda, V. A. (2001). The onset of twinning in metals: A constitutive description. *Acta Materialia*, *49*(19), 4025–4039. https://doi.org/10.1016/S1359-6454(01)00300-7

Noor, S. A., Abdalwahid, K. R., & Ali, H. (2020). Effect of alloying elements on the erosion–corrosion behaviour of Cu-based alloys. *IOP Conference Series: Materials Science and Engineering*, *987*, 012018. https://doi.org/10.1088/1757-899X/987/1/012018

Pike-Wilson, E. A., & Karayiannis, T. G. (2014). Flow boiling of R245fa in 1.1 mm diameter stainless steel, brass and copper tubes. *Experimental Thermal and Fluid Science*, *59*, 166–183. https://doi.org/10.1016/j.expthermflusci.2014.02.024

Rajasekaran, S., Abdulla, Y. A. N., Abdulrahman, A. A. H., et al. (2024). Role of artificial intelligence (AI) and machine learning (ML) in the corrosion monitoring processes. *Zastita Materijala*, *65*(3), 473–480. https://doi.org/10.62638/ZasMat1192

Rajasekaran, S., Yahya Ali, F., & Gunasekaran, V. (2021). Topographical responses of defence grade 7075 Al/TiO2 composite in Red Sea environment. *Materials Today: Proceedings*, *46*(7), 2445–2449. https://doi.org/10.1016/j.matpr.2021.01.358

Ronald, N. C., & Ahmed, S. (2017). Copper alloys: Properties and applications. In *Reference Module in Materials Science and Engineering*. Elsevier. https://doi.org/10.1016/B978-0-12-803581-8.02562-5

Satish, G. K., Srinivas, G., Dongqing, L., et al. (2006). *Heat transfer and fluid flow in mini channels and microchannels*. Elsevier. https://doi.org/10.1016/B978-0-08-044527-4.X5000-2

Sunday, L. L., Sunday, A. A., Tien-Chien, J., et al. (2023). Overview of the impact of heat treatment methods on corrosion performance of metals and alloys. *E3S Web of Conferences*, *390*, 05011. https://doi.org/10.1051/e3sconf/202339005011

Xinyi, L., Yue, J., Zhonghao, J., et al. (2021). Improvement of corrosion resistance of H59 brass through fabricating superhydrophobic surface using laser ablation and heating treatment. *Corrosion Science*, *180*, 109186. https://doi.org/10.1016/j.corsci.2020.109186

Xizhao, L., Lei, K., & Binggong, Y., et al. (2020). Evolution of a superhydrophobic H59 brass surface by using laser texturing via post thermal annealing. *Micromachines*, *11*, 1057. https://doi.org/10.3390/mi11121057

Yahya Ali, F., & Rajasekaran, S. (2020). Investigation on the effect of thermal and mechanical treatment to the offshore corrosion behavior of 6351 aluminum alloy in Red Sea environments. *International Journal of Analytical Chemistry*, *2020*, 8826366. https://doi.org/10.1155/2020/8826366

Zafar, M. N., Rihan, R., & Al-Hadhrami, L. (2015). Effect of $H_2S$ and $CO_2$ in oil/water emulsions on the corrosion resistance of SA-543 steel. *Journal of Materials Engineering and Performance*, *24*, 683–693. https://doi.org/10.1007/s11665-014-1343-7

Zeng, D. L., Chen, G. L., & Shun, C. (2014). Development of research and application of copper alloys with high strength and high conductivity. *Advanced Materials Research*, *1053*, 61–68. https://doi.org/10.4028/www.scientific.net/AMR.1053.61

Zhang, X. K., Yang, X. Y., Chen, W., et al. (2016). Effect of stacking fault energy on mechanical properties and annealing behaviour of brasses. *Journal of Alloys and Compounds*, *679*, 400–407. https://doi.org/10.1016/j.jallcom.2016.04.083